J. Phys. F: Met. Phys. 17 (1987) 1913–1923. Printed in the UK

Densities of states in amorphous Ni–P alloys. Influence of medium-range order

E Belin†, A Traverse‡, A Szász*§ and F Machizaud||

† Laboratoire de Chimie Physique, UA 176, Université Pierre et Marie Curie, 11 rue Pierre et Marie Curie, 75231 Paris Cedex 05, France
‡ CSNSM, Bâtiment 108, BP 1, 91406 Orsay, France
§ Laboratory of Surface and Interface Physics, Eötvös University, Muzéum Krt 6–8, Budapest, Hungary H-1088
|| Laboratoire de Magnétisme, CNRS, 92195 Meudon Principal Cedex, France

Received 19 December 1986

Abstract. We report on soft x-ray studies of the electronic densities of states in amorphous Ni–P alloys prepared by two different techniques, direct current (DC) electrodeposition and implantation. Previous partial results on the distributions of P p and Ni d occupied and unoccupied states are confirmed. New data concerning the filled P s states in various amorphous Ni–P are discussed. The distribution of P p states is compared with that in crystalline Ni_3P. The role of short-range order and medium-range order on the electronic distributions is emphasised.

1. Introduction

Physical properties such as resistivity, magnetism, superconductivity and thermodynamical properties are strongly correlated with electronic structure. This itself depends on atomic arrangement and it has been shown from comparison between amorphous and crystalline systems of the same composition that the lack of long-range order influences the electronic structure (Sénémaud and Costa Lima 1979, Zuckerman *et al* 1981). Likewise, it is important to determine the sensitivity of electronic distributions to modifications in the medium-range atomic structure of amorphous solids of the same nominal composition.

In systems presenting a well defined short-range order, fluctuations may exist in the atomic arrangement at scales greater than two interatomic distances between different amorphous states due to different preparation procedures.

Specific techniques are required to explore scales of the order of three or four interatomic distances around a given atom. Measurements using local probe (nuclear magnetic resonance, Mossbaüer effect, perturbed angular correlation, etc) or diffraction techniques (EXAFS, neutron scattering, etc) provide precise data, on a short scale only, around a given constituent of the alloy. X-ray small angle scattering experiments or resistivity measurements (electronic mean free path of the order of three or four interatomic distances) scale on larger distances but information concerning each

0305-4608/87/091913 + 11 $02.50

constituent is not separated out. Finally, soft x-ray spectroscopy presents the advantage of investigating short- and medium-range order simultaneously, since localised d and more extended s and p states are recorded separately and selectively for each constituent of a system.

In this paper we provide a complete description of the electronic distributions of the valence band and the first empty states in amorphous Ni–P, using soft x-ray emission and absorption spectroscopies (SXES and SXAS). To our knowledge, no complete description of the electronic distributions in such a system has been given, although it is one of the best known from the point of view of transport (Cote 1976, Berrada *et al* 1978, Thomé *et al* 1983, Carini *et al* 1983) and structural properties (Cargill 1970, Sadoc and Dixmier 1976). In Ni–P alloys, a strong chemical bonding of covalent nature between the metalloid atom and the surrounding metal atoms leads to a well defined short-range order around P atoms, similar to that in the amorphous or crystalline alloy (Oelhafen 1983). Partial results for the electronic distributions on electrolytically prepared Ni–P were reported previously (Belin *et al* 1980, 1984). A theoretical band structure calculation (Khanna *et al* 1985) for electronic states is now available for comparison with the experimental results.

Two preparation techniques for the amorphous samples were chosen, different from the electrolytic method used previously (Belin *et al* 1980): DC electrodeposition and ion implantation. They both provide samples with suitable thicknesses for the analysing technique, and are completely different in the method of phosphorus introduction into the nickel matrix. In the implantation case, the phosphorus ion impinges on a high purity Ni target with an incident energy of about 100 keV; this energy is lost during the ion path through the sample by collisions with the host atoms, inducing atomic displacements. Alloying and disordering take place simultaneously. The amorphisation process for a nickel target under phosphorus implantation was followed against the P fluence (Cohen *et al* 1985). This is in contrast with the DC electrodeposition technique in which the phosphorus atoms are codeposited with the nickel atoms, inducing less damage in the target. The radial distribution functions of these samples were determined (Machizaud *et al* 1984). In the following the samples are denoted as Ni–P_i when implanted and Ni–P_e when electrodeposited.

SXES provided P $L_{2,3}$, P Kβ and Ni Lα spectra which give the P s, P p and Ni d distributions respectively of the outer occupied band of both P and Ni in the amorphous alloy and pure elements; SXAS provided the P K and Ni L_{III} spectra which allowed the analysis of the P p and Ni d–s empty states of the alloy and pure elements. X-ray photoelectron spectroscopy (XPS) was used in order to determine the energy positions of the P and Ni inner levels.

From our spectra for pure Ni and from spectra for pure amorphous red P (Belin *et al* 1982) and crystalline Ni_3P (Tanaka and Hiraki 1978), we discuss the influence of chemical and disordering effects.

Our main results are the following. SXS data and theoretical band structure predictions show good agreement for the occupied states distribution. Important features such as the absence of charge transfer, the Fermi level location and the characteristics of interaction between P states and Ni states are established. Another important result comes from the comparison between P spectra from Ni–P_i, Ni–P_e and Ni_3P. In spite of the difference in preparation technique, the short-range order is very similar; however, modifications in the low-lying states of the P distributions are seen, revealing the existence of differences in medium-range order in the amorphous alloys we have studied and the sensitivity of the technique to these differences.

2. Experimental procedure

2.1. Sample preparation

2.1.1. Amorphous implanted films (Ni–P_i). Phosphorus ions were implanted at 300 K, on the Orsay implanter (Chaumont *et al* 1981), into nickel films (800–1000 Å thick) evaporated onto thin Cu or Be plates or onto freshly cleaved NaCl in high vacuum (10^{-8} Torr during evaporation). The incident energies were chosen so as to obtain an homogeneous phosphorus concentration throughout the film depth and the total fluence was of the order of 10^{17} P cm^{-2} to reach a $Ni_{80}P_{20}$ concentrated amorphous alloy. Concentration, homogeneity and purity were checked by Rutherford backscattering experiments while the amorphicity was checked by transmission electron microscopy. These implanted alloys have no gaseous inclusions as in sputtered alloys and no concentration gradient as in melt-spun ribbons.

2.1.2. Amorphous electrodeposited films (Ni–P_e). The samples were prepared by DC electrodeposition from an aqueous buffered solution of nickel acetate and sodium hypophosphite (Fléchon *et al* 1983). By controlling parameters such as the concentration and pH of the solution, the density of the current and, mainly, the electrode potential, it was possible to vary the concentration of P in the sample between 18% and 25%. The depositions were performed either onto bulk copper holders or onto screens of 0.5 μm Al thick covered by 100 Å thick Cu.

2.1.3. Other samples. In order to compare the results from Ni–P with those of the pure elements, bulk nickel or thin evaporated nickel films have also been used and our previous data concerning red amorphous phosphorus (a-P_r) have been taken into account (Belin *et al* 1982).

2.2. Soft x-ray experiments

The spectra were obtained with the help of two vacuum spectrometers equiped with either bent crystals or gratings. Details concerning the spectrographs and experimental methods are given elsewhere (Belin *et al* 1984, Szász *et al* 1984). Let us recall that quartz or beryl ($10\bar{1}1$ and $10\bar{1}0$ planes respectively) crystal spectrometers use the Johann focusing principle and that the Rowland circle of the grating mirror is 2 m radius. An energy resolution of 0.3 or 0.15 eV respectively for P or Ni is available. The accuracy of the energy measurements was about 0.2 eV for P spectra and 0.1 eV for Ni spectra.

The emissive targets were deposited onto Cu or Be holders. Absorption screens were 1000 Å thick Ni–P_i/Be or 450 Å thick Ni–P_e/(Al + Cu) films for the study of the Ni L_{III} spectra. In order to obtain the P K absorption spectrum, we used either a Ni–P_e film of about 5000 Å thick deposited onto an (Al + Cu) holder or a screen obtained from five Ni–P_i films evaporated on to NaCl, separated out onto water and recovered on a Be plate itself covered with a 1000 Å thick Ni–P_i film.

The XPS spectra were induced by the Al Kα radiation excited under 12 kV. The instrumental broadening was 1 eV and the precision on the experimentally determined values of inner levels binding energies was no better than 0.2 eV to 0.3 eV for Ni–P_i and Ni–P_e samples respectively. The binding energies were calibrated, as usual, by taking the Au $4f_{7/2}$ level as 83.8 eV. In order to avoid structural modifications, no argon sputtering-induced cleaning of the samples was performed.

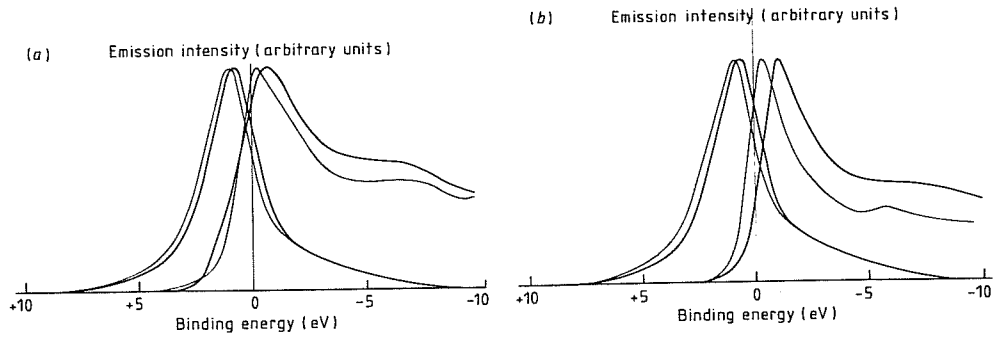

Figure 1. Occupied Ni 3d and unoccupied Ni d–s distributions in amorphous Ni–P_i (*a*) and Ni–P_e (*b*) compared with pure Ni for samples having similar thicknesses. Thick full curves; Ni–P; thin full curves, Ni.

3. Results

Let us underline first that the intensity of the curves presented in the figures are each normalised with respect to their own maximum.

Figure 1 shows Ni 3d distributions both in Ni–P and Ni pure metal. Figure 1(*a*) refers to Ni–P_i (20% P atoms) and figure 1(*b*) to Ni–P_e (21% P atoms). Curves of the same shape and width (not shown here) are obtained from the Ni–P_e samples with other P concentrations. As compared with pure nickel, the Ni Lα distribution, in both Ni–P_i and Ni–P_e, is modified neither in shape nor in width—this is consistent with previous results obtained from electrolytically prepared Ni–P (Belin *et al* 1980)—but it is shifted by +0.2 eV for Ni–P_i and +0.3 eV for Ni–P_e. Within the experimental uncertainties, this accounts for the shift observed for the inner $2p_{3/2}$ level in the alloys with respect to the pure metal (see table 1).

Stronger modifications are seen in the Ni L_{III} empty distribution as compared with pure metal (some of which have already been pointed out previously (Belin *et al* 1980)): (i) a broadening of the distribution in the vicinity edge; (ii) a shift of the top of the curve that also accounts for the shift of the Ni $2p_{3/2}$ inner level; (iii) a spreading and smoothing out of the structure existing at +6 eV from the Fermi level N_F in pure metal; (iv) a fading out of the structure situated at +10 eV from N_F in pure Ni. Notice that the shape of the Ni L_{III} distribution in figure 1(*a*) (Ni–P_i about 1000 Å thick) is slightly different from that in figure 1(*b*) (Ni–P_e about 470 Å thick). It is well known that the shape of the L_{III} white line is strongly influenced by the thickness of the sample (Bonnelle 1966). However this did not affect our comparison between pure metal and Ni–P for each preparation procedure, since the metal and amorphous alloy samples were of same thicknesses and deposited on the same substrates.

Table 1. P $2p_{3/2}$ and Ni $2p_{3/2}$ inner level energies (in eV) in Ni–P and pure elements.

Inner level	Ni/P	Ni–P_i	Ni–P_e
Ni $2p_{3/2}$	852.8	852.7	852.5
P $2p_{3/2}$	130.1	129.3	—

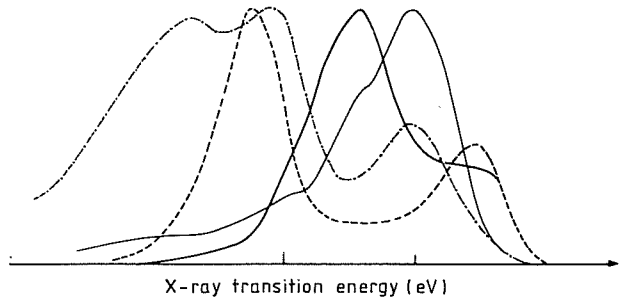

Figure 2. P s and p and Ni d distributions of the valence band and empty P p states for the amorphous Ni–P_i sample. Each curve is normalised with respect to its own maximum. For the discussion of each feature, see text. Thick full curve, P Kβ in Ni–P_i; thin full curve, P Kβ in P; broken curve, P $L_{2,3}$ in Ni–P_i; chain curve, P $L_{2,3}$ in P.

Figure 2 presents the P Kβ and P $L_{2,3}$ emissions in Ni–P_i together with P Kβ and P $L_{2,3}$ emissions corresponding to pure red phosphorous as taken from Belin *et al* (1982) and Wiech (1968).

Figure 3 gives the P p and s distributions of the valence band and empty P p states of Ni–P_i as deduced from P Kβ, P $L_{2,3}$ and P K spectra. The P $L_{2,3}$ emission shows two components C and D which are strongly separated out and are situated on both sides of the principal peak labelled as A of P Kβ, the high energy component D overlapping structure S of P Kβ. Thus both P p and P s distributions are mixed at the top of the valence band and the corresponding edges are superimposed. The P K absorption shows a strong maximum of p empty states, situated just beyond the edge. Ni Lα emission in Ni–P_i, which also overlaps structure S, is reported in this figure.

The energy adjustment of the different distributions has been possible owing to Ni and P inner level measurements as obtained from XPS experiments. The corresponding values are given in table 1 with respect to the Fermi energy level taken as zero energy.

For Ni, the energy adjustment is obtained directly because the x-ray transitions that are studied involve the $2p_{3/2}$ level. For P, the same is true for transitions involving the $2p_{3/2}$ level, namely P $L_{2,3}$. However, for P K transitions, it is necessary to measure the

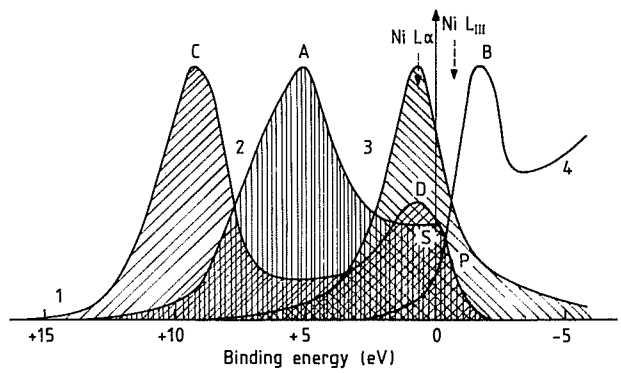

Figure 3. P s and p distributions of the valence band of Ni–P_i compared with a–P_r (taken from Belin *et al* 1982, Wiech 1968). The curves have been adjusted on the x-ray transition energy scale to account for P Kα transition energies. Curves: 1, P $L_{2,3}$; 2, P Kβ; 3, Ni Lα; 4, p K; all in Ni–P_i.

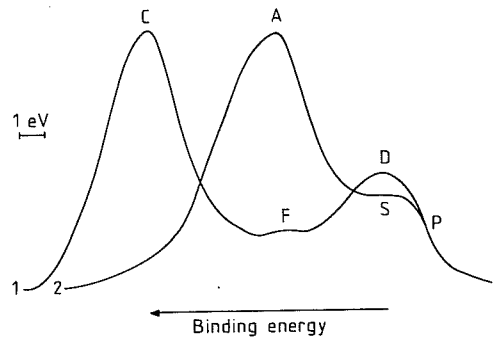

Figure 4. P s and P p distributions in the valence band of Ni–P_e. For the energy adjustment, see text. Curves: 1, P $L_{2,3}$; 2, P Kβ.

P Kα emission line corresponding to $2p_{3/2} \rightarrow 1s$ core level x-ray transition, which was found to be at 2013.7 ± 0.2 eV in Ni–P_i and 2013.9 ± 0.2 eV in all Ni–P_e samples; within the limits of experimental precision, no significant differences are found for this transition energy from one sample to the other. Let us note that previously we have already obtained 2013.7 ± 0.2 eV from amorphous Ni–P alloy as electrolytically prepared and 2013.8 ± 0.2 eV from pure amorphous red P.

The adjustment in the energy scale is obtained within an experimental precision of about ± 0.3 eV.

Such an energy adjustment has not been possible for Ni–P_e samples since, due to surface contaminations, the P $2p_{3/2}$ level could not be measured with sufficient accuracy. We have assumed that the edges of P Kβ and P $L_{2,3}$ are superposed as in Ni–P_i; thus we have obtained the curves shown in figure 4. The general shapes are analogous to those of the curves of figure 2, except there is a small bump denoted F in the P $L_{2,3}$ emission. Let us mention that in P $L_{2,3}$ emission from samples prepared by electrolytic deposition, an additional bump has also been observed at about the same energy range. It has been

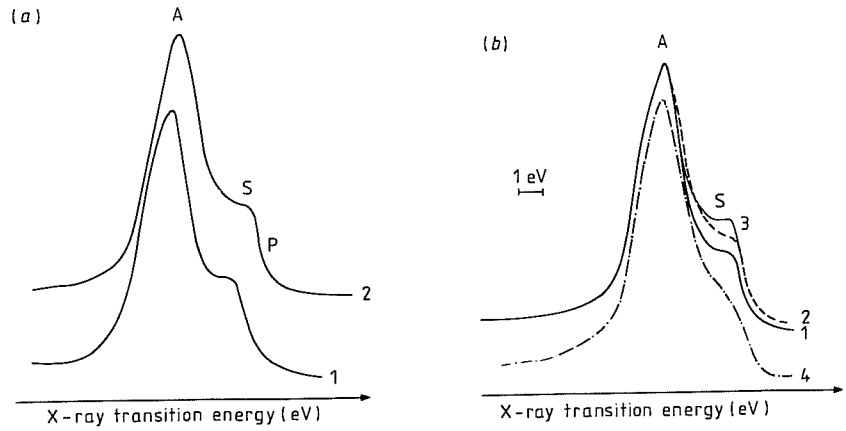

Figure 5. Modification of the P p distributions of the valence band in Ni–P_e: (*a*) plotted against the P concentration; (*b*) plotted against the annealing temperature as compared with Ni–P_i and Ni_3P (from Tanaka and Hiraki 1978). Curves: (*a*) 1, 19.7% P atoms; 2, 25% P atoms; (*b*) 1, annealed; 2, non-annealed; 3, implanted; 4, Ni_3P.

Table 2. P Kβ full width at half maximum (third column), x-ray transition energy of features A, S and P (fourth, fifth and seventh columns) and intensity of structure S as compared with that of peak A (sixth column) in several amorphous Ni–P and crystalline Ni_3P alloys (Tanaka and Hiraki 1978).

Sample	P content	FWHM ± 0.2 eV	A ± 0.2 eV	S ± 0.2 eV	Intensity of S	P ± 0.2 eV
$Ni–P_i$	20%	4.2	2138.0	2142.8	38	2143.2
$Ni–P_e$	19.7%	4.2	2137.2	2141.8	34	2143.0
300 K	25%	4.4	2138.0	2142.8	32	2143.6
$Ni–P_e$	19.7%	4.2	2137.0	2141.6	30	2142.8
annealed	25%	3.8	2137.5	2142.4	27	2143.2
Ni_3P		4.4			19	

ascribed to additional s states due to hydrogen introduced during the preparation procedure (Szász *et al* 1987). The same may be true for the electrodeposited amorphous alloys.

The P Kβ spectra obtained from $Ni–P_e$ samples containing 19.7 and 25% P atoms ($Ni–P_{e(19.7)}$ and $Ni–P_{e(25)}$ respectively) are displayed figure 5(*a*). The energy scale is that of the x-ray transition. Both samples have been annealed at about 375 K and the K β spectra obtained from annealed and non-annealed $Ni–P_{e(25)}$ are given in figure 5(*b*). In this last figure, the summits A that are shifted one with respect to the other (see table 2) have been adjusted at the same energy position. The P Kβ curve which corresponds to $Ni–P_i$ is also presented in figure 5(*b*) within the same adjustment for point A. The general shape of the P Kβ band is the same for all samples. However, one can see from table 2 that slight differences exist in the position of the different features: i.e., in $Ni–P_{e(25)}$ with respect to $Ni–P_{e(19.7)}$, A is shifted by $+0.8 \pm 0.2$ eV, S is shifted by $+1.0 \pm 0.2$ eV and the P Kβ band edge towards high energies (point P in figure 5) is shifted by $+0.6 \pm 0.2$ eV. The intensity of structure S is lowered as P content increases or, for a given amorphous $Ni–P_e$, when the sample is annealed at temperatures below the crystallisation one.

Likewise, in crystalline Ni_3P the shape of the P Kβ distribution is roughly the same as in amorphous Ni–P alloys, but structure S has an intensity markedly lowered with respect to what it is in the amorphous samples (see table 2). The corresponding curve is shown figure 5(*b*), and, in order to be clearer, it has been shifted downwards with respect to the other curves. The adjustment in the energy scale is the same as mentioned above.

4. Discussion

Comparing the occupied electronic distributions in Ni–P and in pure Ni or $a\text{-}P_r$, differences appear in the P distributions revealing a complete modification of the P s and p states. With respect to pure $a\text{-}P_r$, in the Ni–P alloys: (i) the high-lying quasi-s pure states are concentrated in a narrower energy range (about 6 eV against 12 eV in $a\text{-}P_r$) due to purer character, (ii) all the same, the middle lying p states arise purer in character, (iii) sp hybridised states are present at the very top of the valence band and cover an energy range of about 2.5 eV. By contrast, we observe no modification in the shape and width of the Ni 3d distribution except for a small energy shift which is also observed in the Ni 3d empty states. The Ni 4s distribution could not be obtained separately; it is present in the same energy range as the Ni 3d distribution, but, due to transition probabilities, the

corresponding intensity is too low with respect to the intensity of transitions from 3d states to be clearly observable.

Within the limits of experimental precision, there is thus a fair overlap between Ni 3d–4s and P hybridised sp occupied states. The present results concerning occupied states in the amorphous alloys added to the previous conclusions (Belin *et al* 1980, 1984) confirm that amorphisation of Ni through P incorporation leads to an admixing of P sp-hybridised states with Ni extended states, the other P states acquiring s or p quasi-pure character.

In the empty states we also observe an overlap between Ni 3d and P p states. No charge transfer occurs from P to Ni, as, in this case, a strong modification of the Ni d empty band should have resulted.

Similar trends were found for the electronic distributions in other amorphous metal–metalloid alloys NiB (Belin *et al* 1981), FeB (Paul and Neddermeyer 1985, De Crescenzi *et al* 1983), FeNiB (Hricovini and Krempasky 1985), NiPtP (Choi *et al* 1985), showing clearly that the d band is insensitive to the lack of long-range order, due to its localised nature, while the sp states, particularly of the metalloid atom, are mostly affected by the chemical disorder.

This is in contrast to the interpretation of at least three recent experiments on infrared reflectivity and Hall effect measurements (McKnight and Ibrahim 1984) and low temperature specific heat studies on Ni–P (Kuentzler *et al* 1985) which led to the conclusion that the Ni d band is filled with electrons given by the metalloid, like in a rigid band model.

The experimental electronic distributions for $Ni_{80}P_{20}$ we have obtained, can be compared with band structure calculations. A calculation based on the use of the Korringa–Kohn–Rostoker potential approximation was performed by Khanna *et al* (1985) on the $Ni_{74}P_{26}$ alloy; the density of states they have obtained is presented in figure 6. The corresponding curve displays a three peaked shape which is consistent with the experimental distributions as shown in figure 2. Let us recall that in the experimental case each curve is normalised with respect to its own maximum, so intensities are not directly comparable with those of calculations.

No charge transfer is predicted by this calculation in conformity with our results. Table 3 shows a direct comparison between our soft x-ray data presented in figure 2 and the different band energies given in figure 6. SXS measurements and theoretical predictions (Khanna *et al* 1985) agree in shape but the theoretical curve is more spread out, this may arise from the values of theoretical parameters involved in the calculation or from the difference in the P concentration.

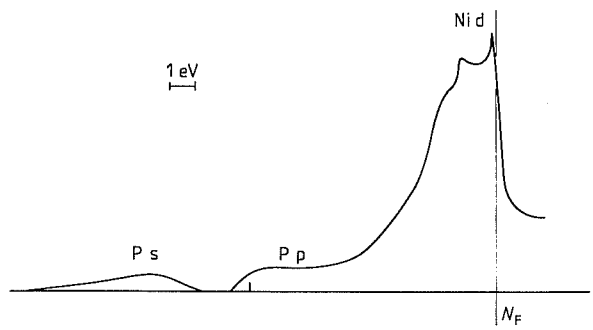

Figure 6. Calculated electronic density of states in amorphous $Ni_{74}P_{26}$ obtained by Khanna *et al* (1985).

Table 3. Energy of the experimental features of Ni–P_i as compared with the calculation performed by Khanna *et al* (1985) for $Ni_{74}P_{26}$ alloy. Energies (in Ryd), are referred to the Fermi level taken as zero energy.

	Ni d band		P 3s states		P 3p states
	Mean energy	FWHM compared with pure Ni	Lowest energy	Mean energy	Mean energy
$Ni_{80}P_{20}$ (expt)	−0.06	Unchanged	−1.10	−0.7	−0.39
$Ni_{74}P_{26}$ (calc.)	−0.10	Slightly decreased	−1.27	−0.9	−0.47

Using the Haydock recursion method, the electronic states distribution of other amorphous metal–metalloid alloys—Fe_xP_{1-x} and Fe_xB_{1-x}—(Fujiwara 1982, 1984) was calculated which exhibit similar features concerning the states mixing, charge transfer, location of the Fermi level and the shape of the density of states than the results of Khanna *et al* (1985).

Another result can be drawn from the differences in the P sp electronic distributions compared with the preparation procedure or thermal treatment as reported in figure 5(*a*) and (*b*) and table 2.

Those differences essentially concern structure S which arises from the hybridised sp states located at the top of the valence band. As generally admitted (Güntherodt *et al* 1980), we can consider that the short-range order (or local order) is the same for all Ni–P amorphous alloys and crystalline Ni_3P. During relaxation of amorphous Ni–P induced by annealing, the mean short-range order remains the same, only medium-range order is affected, metastable sites being eliminated (Waseda and Miller 1978, Machizaud *et al* 1984). Then, as the sp hybridised states are spatially delocalised, structure S characterises medium-range order and differences in S intensity imply differences in the medium-range order. These sp hybridised states appear with less contrast the more the sample is chemically and topologically ordered. So, in view of these results, it is possible to determine the more disordered sample. From the comparison between Ni–P_i and Ni–P_e, since structure S is of higher intensity in the former case, we suggest that Ni–P_i is more disordered than Ni–P_e of the same P concentration. Indeed, the atomic arrangement may not be the same in the implanted and the electrodeposited alloys, on a range which is larger than the short-range one, but it is not possible to get more precise information on the atomic arrangement.

Indications can be given by other experimental results which are consistent with these observations. We must notice that the implantation technique itself implies a high level of disorder due to the damage created by the incident ion along its path: typically about 500 Ni atoms are displaced from their sites by an incident phosphorus ion. X-ray small-angle scattering on amorphous $Pd_{80}Si_{20}$ prepared by ion implantation shows that crystallisation takes place at a lower temperature than in a quenched alloy (Naudon and Traverse 1985). This behaviour looks like that of a sputtered alloy. From specific heat masurements (Garoche 1981), it was shown that a sputtered glass is less homogeneous than a quenched one. Okamoto and Fukushima (1984) and Lashmore *et al* (1982) have seen different Ni environments in electrolytical, electrodeposited and in rapidly quenched

Ni–P which contrasts with a former conclusion by Suzuki *et al* (1978). Further evidence in favour of higher disorder at medium-range scale in implanted glasses is provided by the value of the recombination volume deduced from the resistivity fluence dependence under irradiation. This volume, inside which a displaced atom spontaneously recombines with its own vacancy, is two times smaller in an implanted $Pd_{80}Si_{20}$ than in the same alloy prepared by melt spinning (Traverse *et al* 1984). This indicates that, due to higher degree of disorder, the displaced atom in an implanted alloy has to be nearer to its vacancy to be able to recombine with it. The recombination volume values (88 atomic volumes for the melt-spinning prepared $Pd_{80}Si_{20}$ and 46 atomic volumes for the implanted one) provide radii values of 2.8 and 2.2 interatomic distances respectively. So this is inside a torus whose radii values are between about two and three interatomic distances where the atomic arrangement is different from one sample to the other (hence between about 5 and 8 Å in Ni–P, by taking an interatomic distance of 2.5 Å). This represents what we have called the medium-range scale and may be an evaluation of the sensitivity of the SXS method as applied to amorphous Ni–P.

5. Conclusion

Complete measurements on the electronic distributions in the amorphous alloy Ni–P have confirmed that the lack of medium- and long-range order does not influence states already partially localised in pure elements.

No charge transfer occurs from P to Ni atoms; hybridised P sp states are present at the very top of the valence band and are mixed with Ni 3d–4s states. There is quite good agreement with a recent calculated electronic density of states for the amorphous alloy $Ni_{74}P_{26}$ (Khanna *et al* 1985).

From the point of view of the preparation procedure, despite the damage it introduces in the material, implantation is one of the most relevant techniques for preparing alloys of good purity, provided that the vacuum is high enough during evaporation of the target and during the implantation process itself.

Our present and previous results obtained on samples prepared by different techniques (DC electrodeposition, implantation and electrolytic) compared with crystalline Ni_3P alloy show that the P hybridised sp states located at the top of the valence band are very sensitive to disorder since clear differences are seen from one sample to the other. This comes from the fact that these sp hybridised states are more delocalised than the other states, so they are sensitive to medium-range order interactions. We attribute the modifications seen in P sp distributions when passing from one sample to the other to differences in the medium-range order, say an order involving two to four interatomic distances.

Finally, from our results, SXS is confirmed to be of interest for the investigation of the electronic distributions of alloys of the same nominal concentration but presenting differences in the medium-range order.

Acknowledgments

J Chaumont and F Lalu are gratefully acknowledged for their help during the P implantation. We particularly thank C Bonnelle, H Bernas and P Nedellec for their constructive remarks on the manuscript.

References

Belin E, Bonnelle C, Fléchon J and Machizaud F 1980 *J. Non-Cryst. Solids* **41** 219
Belin E, Bonnelle C, Zuckerman S and Machizaud F 1984 *J. Phys. F: Met. Phys.* **14** 625
Belin E, Kuhnast F A and Fléchon J 1981 Communication to *Congrès de la Société Française de Physique, Clermont-Ferrand*
Belin E, Sénémaud C and Zuckerman S 1982 *Solid State Commun.* **44** 413
Berrada A, Lapierre M F, Loegel B, Panissod P and Robert C 1978 *J. Phys. F: Met. Phys.* **8** 845
Bonnelle C 1966 *Ann. Phys., Paris* **1** 1
Cargill G S III 1970 *J. Appl. Phys.* **41** 12
Carini J P, Nagel S R, Varga L K and Schmidt J 1983 *Phys. Rev.* B **27** 7589
Chaumont J, Lalu F, Salomé M, Lamoise A M and Bernas H 1981 *Nucl. Instrum. Meth.* **189** 193
Choi M, Pease D M, Hines W A, Hayes G H, Budnick J I, Heald S M, Hasegawa R and Schone W E 1985 *Phys. Rev.* B **32** 7670
Cohen C, Benyagoub A, Bernas H, Chaumont J, Thomé L, Berti M and Drigo A V 1985 *Phys. Rev.* B **31** 5
Cote P J 1976 *Solid State Commun.* **18** 1311
De Crescenzi M, Colavita E, Papagno L, Chiarello G, Scarmozzino R, Caputi L S and Rosei R 1983 *J. Phys. F: Met. Phys.* **13** 895
Fléchon J, Mbemba G, Machizaud F and Kuhnast F A 1983 *J. Chim. Phys.* **80** 391
Fujiwara T 1982 *J. Phys F: Met. Phys.* **12** 661
—— 1984 *J. Non-Cryst. Solids* **61–62** 1039
Garoche P 1981 *PhD thesis* Paris XI University (unpublished)
Güntherodt H J *et al* 1980 *J. Physique Coll.* **41** C8 381
Hricovini K and Krempasky J 1985 *J. Phys. F: Met. Phys.* **15** 1321
Khanna S N, Ibrahim A K, McKnight S W and Bansil A 1985 *Solid. State Commun.* **55** 223
Kuentzler R, Bakonyi I and Lovas A 1985 *Solid State Commun.* **55** 567
Lashmore D S, Bennett L H, Schone H E, Gustafson P and Watson R E 1982 *Phys. Rev. Lett.* **48** 1760
Machizaud F, Kuhnast F A and Fléchon J 1984 *J. Non-Cryst. Solids* **68** 271
McKnight S W and Ibrahim A K 1984 *J. Non-Cryst. Solids* **61–62** 1301
Naudon A and Traverse A 1985 Private communication
Oelhafen P 1983 *Glassy Metals II, Topics in Applied Physics* vol 53 (Berlin: Springer) p 283
Okamoto T and Fukushima Y 1984 *J. Non-Cryst. Solids* **61–62** 379
Paul Th and Neddermeyer H 1985 *J. Phys. F: Met. Phys.* **15** 79
Sadoc J F and Dixmier J 1976 *Mat. Sci. Engng* **23** 187
Sénémaud C and Costa Lima M T 1979 *J. Non-Cryst. Solids* **33** 141
Suzuki K, Itoh F, Fukunaga T and Honda T 1978 *Rapidly Quenched Metals II* vol 2 ed. B Canton p 410
Szàsz A, Kojnok J, Kertesz L, Paàl Z and Hegedüs Z 1984 *Thin Solids Films* **116** 279
Szàsz A, Kojnok J and Belin E 1987 to be published
Tanaka K and Hiraki A 1978 *Japan. J. Appl. Phys.* **17** 1214
Thomé L, Traverse A and Bernas H 1983 *Phys. Rev.* B **28** 6523
Traverse A, Audouard A, Fan X J, Chaumont J and Bernas H 1984 *Radiat. Eff.* **81** 255
Waseda Y and Miller W A 1978 *Phys. Status Solidi* **49** K31
Wiech G 1968 *Z. Phys.* **216** 472
Zuckerman S, Belin E, Sénémaud C, Thèye M L and Gheorghiu A 1981 *Inner-Shell and X-Ray Physics of Atoms and Solids* ed. D Fabian (New York: Plenum) p 585